© 2018. Published by The Company of Biologists Ltd | Journal of Experimental Biology (2018) 221, jeb189167. doi:10.1242/jeb.189167

RESEARCH ARTICLE

Transforming growth factor-β1 induces differentiation of rainbow trout (*Oncorhynchus mykiss*) cardiac fibroblasts into myofibroblasts

Elizabeth F. Johnston and Todd E. Gillis*

ABSTRACT

The collagen content of the rainbow trout heart increases in response to cold acclimation and decreases with acclimation to warm temperatures. This ability to remodel the myocardial extracellular matrix (ECM) makes these fish useful models to study the cellular pathways involved in collagen regulation in the vertebrate heart. Remodelling of the ECM in the mammalian heart is regulated, in part, by myofibroblasts which arise from pre-existing fibroblasts in response to transforming growth factor-β1 (TGF-β1). We have previously demonstrated that treatment of cultured rainbow trout cardiac fibroblasts with human TGF-β1 causes an increase in collagen production. Here, we showed that repetitive treatment of rainbow trout cardiac fibroblasts with a physiologically relevant concentration of human recombinant TGF-β1 results in a ∼29-fold increase in phosphorylated small mothers against decapentaplegic 2 (pSmad2); a 2.9-fold increase in vinculin protein, a 1.2-fold increase in cellular size and a 3-fold increase in filamentous actin (F-actin). These are common markers of the transition of fibroblasts to myofibroblasts. Cells treated with TGF-β1 also had highly organized cytoskeletal α-smooth muscle actin, as well as increased transcript abundances of *mmp-9*, *timp-2* and *col1a1*. Furthermore, using gelatin zymography, we demonstrated that TGF-β1 treatment causes a 5.3-fold increase in gelatinase activity. Together, these results suggest that trout cardiac fibroblasts have the capacity to differentiate into myofibroblasts and that this cell type can increase extracellular collagen turnover via gelatinase activity. Cardiac myofibroblasts are, therefore, likely involved in the remodelling of the cardiac ECM in the trout heart during thermal acclimation.

KEY WORDS: Cardiac remodelling, Extracellular matrix, Phenotypic plasticity, TGF-β1

INTRODUCTION

Rainbow trout remain active in waters where temperatures vary seasonally between 4°C and 21°C, indicating that the cardiovascular system remains functional across this range of temperatures. Cold acclimation of trout results in an increase in muscle fibre bundle size within the myocardium, as well as an increase in extracellular collagen deposition (Keen et al., 2016, 2017; Klaiman et al., 2011). Conversely, warm acclimation of trout causes ventricular atrophy and a decrease in extracellular collagen. It is thought that these changes to the heart help to maintain cardiac function during large changes in temperature (Keen et al., 2016, 2017; Klaiman et al., 2011). This also suggests that trout living in a temperate environment undergo annual cycles of myocardial ECM remodelling. In addition, the apparent ease with which the collagen content of the trout heart changes in response to thermal acclimation makes these animals potentially useful models to study the mechanisms regulating connective tissue deposition and removal in the vertebrate heart under physiological conditions.

An important regulator of collagen deposition in the mammalian heart is the cytokine transforming growth factor-β1 (TGF-β1). TGF-β1 activates mitogen activated kinase (MAPK) and small mothers against decapentaplegic (Smad) pathways, which translocate a ligand signal into the nucleus via cofactors, activating transcriptional factors on genes, and results in increased collagen protein in the ECM (Lee et al., 2002; Nakao et al., 1997; Nyati, 2012). We have recently demonstrated that the treatment of cultured rainbow trout cardiac fibroblasts with TGF-β1 stimulates collagen deposition, suggesting that the role of this cytokine in the heart is conserved in trout (Johnston and Gillis, 2017).

In the mammalian heart, a second role of TGF-β1 is to initiate the transformation process by which fibroblasts become myofibroblasts (Vaughan et al., 2000). Myofibroblasts are intermediate to fibroblasts and smooth muscle cells, as this cell type is able to both produce collagen and contract, as a result of α-smooth muscle actin (α-SMA) within in the cytoskeleton (Lighthouse and Small, 2016). These capabilities allow myofibroblasts to close an injury via contraction, and then establish a scar with deposited collagen (Darby et al., 2014). In addition to expressing extracellular collagen, myofibroblasts also produce matrix metalloproteinases (MMPs) (Darby et al., 2014). MMPs are a family of zinc-dependent endopeptidases that are collectively able to digest all types of connective tissue (Visse and Nagase, 2003). By producing both collagen and MMPs, myofibroblasts play a critical role in controlling, and remodelling, the myocardial ECM (Klingberg et al., 2013; Ma et al., 2014). For example, during the onset of heart disease in mammals, myofibroblasts are thought responsible for the increase in myocardial stiffness (Darby et al., 2014; Tomasek et al., 2002). As cold acclimation increases the stiffness of the trout ventricle (Keen et al., 2016), it is possible that this cell type also plays a role in this remodelling response (Gillis and Johnston, 2017). However, it is not known if myofibroblasts can arise from pre-existing fibroblasts in the rainbow trout heart. While studies of the regenerating zebrafish heart have demonstrated the presence of myofibroblasts (Gonzalez-Rosa et al., 2011), no studies have examined the role of TGF-β1 in regulating their phenotype.

In zebrafish, a population of myofibroblasts appears in the myocardium 3 days after cardiac injury, and the number of these cells peaks at 21 days, then disappears by 90 days (Gonzalez-Rosa et al., 2011). This suggests that these cells play a role in the regenerative process. Interestingly, Chablais and Jazwinska (2012) demonstrated that blocking the TGF-β1 signal following cardiac injury in zebrafish inhibits regeneration (Chablais and Jazwinska,

Department of Integrative Biology, University of Guelph, Guelph, ON N1G-2W1, Canada.

*Author for correspondence (tgillis@uoguelph.ca)

T.E.G., 0000-0002-8585-0658

Received 23 July 2018; Accepted 29 October 2018

2012). This suggests that the conversion of fibroblasts into myofibroblasts, likely triggered by TGF-β1, may be involved in cardiac regeneration. Furthermore, TGF-β1 induces a transient matrix of collagen types I and XII during zebrafish cardiac regeneration, indicating that this cytokine plays a role in the reparative process (Marro et al., 2016). However, there are limited data demonstrating that TGF-β1 induces fibroblasts to differentiate into myofibroblasts in any fish cell line.

The hypothesis that will be tested in the current study is that TGF-β1 stimulates the conversion of trout cardiac fibroblasts into myofibroblasts. To investigate this, we treated cultured trout cardiac fibroblasts with TGF-β1 and then examined a number of molecular and cellular responses that are indicative of their conversion into myofibroblasts. More specifically, we examined activation of the Smad2 pathway, changes in cellular morphology, the gene transcripts and enzymatic activity of MMPs, as well as expression of F-actin, α-SMA and vinculin (an actin anchoring protein).

MATERIALS AND METHODS

Cell culture

Fibroblast cells were isolated from male rainbow trout [*Oncorhynchus mykiss* (Walbaum 1792)] ventricles and kept under conditions as previously described (Johnston and Gillis, 2017). Four cell lines, generated from the cardiac ventricles of four different fish, were maintained at 21°C in Leibovitz's L-15 medium with 1% penicillin-streptomycin, 1% amphotericin B and 10% fetal bovine serum (FBS), hereafter referred to as whole medium, and split 1:2 during passaging. Fibroblasts used in the experiments described below were between passages 17 and 22. Experiments were conducted in triplicate, this means that three of the four cell lines were used in each experiment.

Inducing fibroblast differentiation

Fibroblasts were treated with TGF-β1 as described by Khouw et al. (1999) to determine if this cytokine causes rainbow trout fibroblasts to differentiate into myofibroblasts. In brief, 3×10^4–1×10^5 cells were grown on acid-etched coverslips or ∼2×10^6 cells were grown in 75 cm^2 flasks and exposed to 15 ng ml^{-1} TGF-β1 (R&D Systems) for 7 days (Khouw et al., 1999). TGF-β1 was replenished every other day, i.e. day 0, 2, 4, 6 to maintain activation of the differentiation pathway (Khouw et al., 1999). The second treatment group was cells that were treated with 15 ng ml^{-1} basic fibroblast growth factor (bFGF; Invitrogen, Carlsbad, United States) on the same days that TGF-β1 was added to the first treatment group. FGF inhibits differentiation and was therefore used as a comparison with the cells treated with TGF-β1 (Jester et al., 1996; Khouw et al., 1999; Mattey et al., 1997; Ronnov-Jessen and Petersen, 1993).

Immunocytochemistry

After 7 days, cells were fixed in 4% paraformaldehyde and permeabilized with phosphate buffered saline (PBS)+0.1% Tween 20 (Fisher Scientific, Hampton, United States) (PBST) and blocked with 1% goat normal serum in PBST for 1 h before application of 1:500 monoclonal mouse anti-α-smooth muscle actin (Sigma-Aldrich, #A2547) overnight at 4°C. The next day, cells on coverslips were washed and 1:500 polyclonal goat anti-mouse Alexa Fluor 488 (ThermoFisher Scientific, #A10680) was added for 1 h at room temperature.

Filamentous actin staining

For visualization of total filamentous actin (F-actin), the cells were stained with 100 nmol l^{-1} acti-stain 488 phalloidin (Cytoskeleton Inc., #PHDG1) for 30 min and counterstained with 1 µmol l^{-1} DAPI (Sigma-Aldrich), mounted in ProLong Gold Antifade Mountant (ThermoFisher Scientific) and sealed with clear nail polish.

Western blotting and phospho-blotting

Cells in the control and treatment groups were washed with 5 ml PBS, then 200 µl radioimmunoprecipitation assay (RIPA) buffer containing 1 µmol l^{-1} phenylmethane sulfonyl fluoride (PMSF, Sigma) and phosphatase inhibitors (50 mmol l^{-1} sodium fluoride, 5 mmol l^{-1} sodium pyrophosphate and 5 mmol l^{-1} sodium orthovanadate), then incubated on wet ice for 5 min. Cells were removed from flasks by scraping and then transferred to a 1.5 ml Eppendorf tube and homogenized by being repeatedly flushed through a needle and syringe, on ice. The lysate was then maintained at 4°C with gentle agitation for 30 min, centrifuged for 20 min at 20,000 ***g***, and the supernatant was reserved and measured for protein content using a bicinchoninic acid (BCA) assay (Bio-Rad, Hercules, United States). A 20–30 µg sample of protein was loaded into the lane of a 6% (vinculin, collagen) or 12% (pSmad2, Smad2) polyacrylamide gel and run at 160 V for ∼1–1.5 h. Proteins were electro-blotted onto a polyvinylidene fluoride membrane with wet transfer at 30 V for 16 h at 4°C, blocked in either 5% skimmed milk powder or 5% bovine serum albumin (BSA; Bioshop, Burlington, Canada) in Tris-buffered saline with 0.1% Tween 20 (TBST) (hereafter referred to as blocking buffer) for 1 h at room temperature then incubated in 1:1000 monoclonal mouse anti-vinculin (R&D Systems, #MAB6896), 1:1000 polyclonal rabbit anti-salmon collagen type I (Cedarlane, Burlington, Canada, #CL50171AP), or goat 1:1000 monoclonal rabbit anti-pSmad2(Ser465/467)/Smad2 (Cell Signaling Technology, #138D4/D43B4) in blocking buffer plus 0.05% sodium azide overnight at 4°C. The next day, blots were incubated in goat anti-mouse biotinylated secondary or goat anti-rabbit IgG-HRP secondary antibody buffer (Santa Cruz Biotechnology) at a dilution of 1:1000 in blocking buffer. After removal of biotinylated secondary antibody, a Vectastain kit (Vector Labs) diluted in blocking buffer was used to conjugate HRP prior to visualization. An Amersham ECL Plus detection kit (GE Healthcare) was used as per the manufacturer's instructions to induce chemiluminescence, which was subsequently visualized with the ChemiDoc MP imaging system (Bio-Rad). Data from blots were compared with whole protein content by running a parallel gel of identical protein and loading volumes and staining with Coomassie Blue (Bio-Rad) to quantify total protein of samples (Eaton et al., 2013). An inter-assay control composed of several randomly selected samples was run in every gel to ensure that blots were comparable; the densitometry of this control did not vary from membrane to membrane.

Quantification of cellular size and total filamentous actin

Images of cells post-treatment were imaged using a Nikon Eclipse 90i microscope equipped with a 12-bit colour digital camera (Q-Imaging). Coverslips with phalloidin-stained cells were separated into 9 distinct regions and pictures of cells were randomly acquired within each region. Exposure time for phalloidin or DAPI filters were identical for all slides. The DAPI and phalloidin–actin images were first overlaid to determine where whole cells were present in the field of view (FOV). Images with only actin fluorescent present were converted to 8-bit (greyscale) and regions of interest (ROIs) containing individual or clusters of cells were selected based on several criteria including: (1) the cells are wholly intact, e.g. nuclei and cytoskeletons undamaged; (2) no part of the cell was outside the

F.O.V.; and (3) the boundaries of the cell(s) was discernible so that ROIs contain an accurate actin content measurement. A box was drawn just beside the ROI and measured for background fluorescent noise, which was used to correct the mean grey value (MGV) for each ROI. Actin quantification is expressed as background-corrected MGV per cell within the ROI. The average area (μm^2) of the cells was also quantified as myofibroblasts are larger than regular fibroblasts (Masur et al., 1996; Sun and Weber, 1996). This measurement involved dividing the total area of the ROI by the number of cells within the ROI. The fluorescence of each cell was also divided by the area of the cell to determine the relative fluorescence per μm^2.

Gelatin zymography

MMP activity was assessed using a modified protocol from Lødemel and Olsen (2003). In brief, fibroblasts were grown in 75 cm^2 flasks and kept in normal whole medium, or treated every 48 h with bFGF or TGF-β1 for 7 days. After this time, fibroblasts were incubated in L-15 medium without FBS for 24 h, as serum contains gelatinases that would interfere with accurate endogenous MMP activity. Spent medium was reserved so that MMP activity could be later determined, and then cells were collected from the flasks by adding lysis buffer with protease inhibitors (50 mmol l^{-1} Tris-HCl, pH 7.4, 10 mmol l^{-1} $CaCl_2$, 0.05% Brij 35, 0.2 g l^{-1} NaN_3, 1 mmol l^{-1} PMSF, 1 mmol l^{-1} benzamidine) to the flask followed by scraping. Samples were diluted 10-fold for protein measurement using a BCA assay. 20 µg of total non-reduced and non-heated protein was dissolved in modified Laemmli buffer (62.5 mmol l^{-1} Tris-HCl, pH 6.8, 40 g l^{-1} SDS, 250 ml l^{-1} glycerol and 10 g l^{-1} Bromophenol Blue) (Lødemel and Olsen, 2003) and then loaded into the lanes of a 9% polyacrylamide gel co-polymerized with 0.2% (w/v) gelatin. This gel was run for 1.5 h at 150 V at 4°C alongside a regular 9% polyacrylamide gel with identical samples. The samples in the regular polyacrylamide gel served as a normalization standard (Eaton et al., 2013) (Fig. S2). Once run, the gelatin-polyacrylamide gels were washed 3 times for 20 min each in 2.5% Triton X-100 at room temperature. These gels were then incubated in renaturing buffer (50 mmol l^{-1} Tris-HCl, pH 8.0, 10 mmol l^{-1} $CaCl_2$, 0.2 g l^{-1} NaN_3 and 1.0 µmol l^{-1} $ZnCl_2$) for 36 h at 38°C (Lødemel and Olsen, 2003). The next day, gels were stained in 1.0 g l^{-1} Coomassie Brilliant Blue in 450 ml l^{-1} methanol and 100 ml l^{-1} acetic acid and destained in 100 ml l^{-1} methanol and 100 ml l^{-1} acetic acid (Lødemel and Olsen, 2003). Zymogram gels and total protein gels were imaged in a ChemiDoc MP imaging system (Bio-Rad) under Coomassie settings.

Quantitative real-time PCR

The transcript abundance of genes associated with connective tissue regulation was quantified in cardiac fibroblasts after 7 days of bFGF or TGF-β1 treatment and in untreated control cells. Total RNA was extracted from fibroblasts using Trizol (ThermoFisher Scientific) on ice according to the manufacturer's instructions and quantified using a Nanodrop 8000 (ThermoFisher Scientific). A 1 µg sample of total RNA was treated with DNase I (Sigma) and used to synthesize cDNA with the High Capacity cDNA Synthesis Kit (ThermoFisher Scientific) following the manufacturers' instructions. Duplicate cDNA reactions in which the Multiscribe RT enzyme was omitted were included for 10% of total samples, chosen randomly, to verify the efficacy of the DNase treatment. Transcript abundance was measured in duplicate reactions on a CFX96 Real-Time PCR Detection System (Bio-Rad) using default cycling conditions and a dissociation cycle. Each 15 µl reaction contained 1×Power SYBR Green Master Mix (ThermoFisher Scientific), 200 nmol of each gene-specific primer (Table 1) and 1:15 v:v cDNA. Custom oligos for *col1a1*, *timp-2*, *mmp-2* and *β-actin* were designed using Primer3. The sequence of the gene-specific primers for *mmp-9* was that used by Keen et al. (2016). All reactions generated a single-peaked dissociation curve at the predicted amplicon melting temperature. The mRNA abundance was quantified by fitting the threshold cycle to the antilog of standard curves prepared from serially diluted cDNA. Isoform transcript abundance was normalized to *β-actin*. The transcript level of this housekeeping gene did not change in response to TGF-β1 or bFGF treatment. All primers used had an efficiency of 80–110%. All non-reverse transcribed control samples failed to amplify.

Statistical analyses

All data were initially subjected to a Shapiro–Wilk test for normality. Any data that failed to meet normality were log-transformed prior to analysis. All data were tested with a one-way ANOVA and *post hoc* Bonferroni correction, where significance at 95% confidence was detected for both tests. The *n*-values shown for western blots, zymography and qPCR represent either established fibroblasts from the hearts of different fish, or a fibroblast line from the same fish maintained in separate passages, cryopreserved on a different passage number and day, and thawed for experiments on different days. The *n*-value for immunocytochemistry image analysis represents one individual cell from one of three cell lines, except for the F-actin-stained cells, where averages are representative of n=80–110 individual cells examined.

RESULTS

Smad2 activation

The level of Smad2 phosphorylation in TGF-β1-treated cells was 28.6-fold greater than that of control cells, and 17-fold greater than that of bFGF-treated cells (P<0.05, Fig. 1). There was no difference in the level of Smad2 phosphorylation between control and bFGF

Table 1. Forward and reverse primer sequences used in quantitative real-time PCR to amplify rainbow trout gene transcripts

Gene	Sequence (5′–3′)	Amplicon	Accession no.	Efficiency (%)	R^2
β-actin	F: ACACCCGACTACCACTTCAG R: GACTGAGAAGCTGGGTTTGG	96	AF157514.1	84	0.99
mmp-2	F: AGACGCATAGACGCTGGCTAA R: GCAGGATAGGCTGGTTGGATAG	78	AB021698.1	95	1
mmp-9	F: ACCCCTTCGATGGTAAGGAC R: GGTCCAGTTTTCGTCATCGT	98	AJ320533.1	100	0.99
timp-2	F: AGCGCCCCAGAGGAGTGT R: ACCGCTGTGGCTCTTTTCC	57	AY606030.1	102	0.99
col1a1	F: CCCGAGCCATGCCAGAT R: CGGATGTGTCCTCGCAGATAA	76	NM_001124177.1	90	0.99

Journal of Experimental Biology (2018) 221, jeb189167. doi:10.1242/jeb.189167

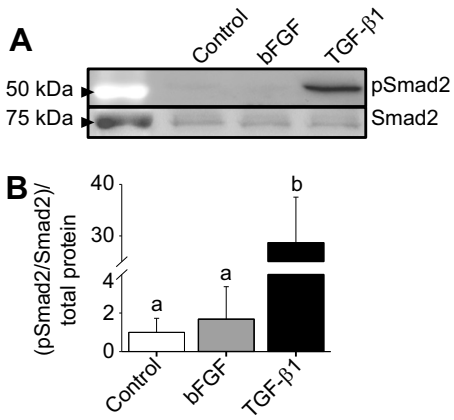

Fig. 1. The effect of bFGF and TGF-β1 on Smad2 phosphorylation in cultured trout cardiac fibroblasts. Cardiac fibroblast cultures were treated with medium alone or medium containing 15 ng ml^{-1} bFGF or 15 ng ml^{-1} TGF-β1 every 48 h for 7 days and total Smad2 and phosphorylated Smad2 were quantified using western blotting and densitometry. (A) Representative western blot image for pSmad2 and Smad2 acquired from the same cell line. This experiment was repeated three times with different cell lines (from different fish) and both Smad2 and pSmad2 blots were acquired from the same membrane. The images here are a composition of blots from the specific HRP-conjugated antibody and Cy5 ladder image, resulting in a dark grey background. The 75 kDa marker became dark after membrane stripping. (B) Mean pSmad2 and Smad2 levels measured by densitometry and standardized to total protein. Phosphorylated Smad2 was first standardized to total Smad2 before normalizing to total protein (Fig. S1). Differences were detected using a one-way ANOVA with *post hoc* Bonferroni correction. Different letters denote an effect of treatment on phosphorylation level of Smad2, relative to control (P<0.05). Note the large break on the *y*-axis. The *n* for each experiment is 3, with each *n* being a protein sample extracted from cultured cells derived from a different trout ventricle.

treatments (P>0.05, Fig. 1). Total Smad2 protein was unchanged between all three groups (P>0.05, Fig. 1A).

Effect of TGF-β1 treatment on actin and cell size

In comparison to control (Fig. 2A), samples treated with bFGF contained more fibroblasts (Fig. 2B). Fibroblasts treated with TGF-β1 had large cytoskeletons with dense F-actin fluorescence (Fig. 2C). Repeated treatment of fibroblast cultures with TGF-β1 induced an increase in total F-actin content per cell (Fig. 2D) and an increase in average cell size (Fig. 2E) (P<0.05). The average amount of actin per cell in the TGF-β1-treated fibroblasts was 58% and 75% greater than that of bFGF-treated and control cells, respectively (P<0.05, Fig. 2D). Cells treated with bFGF expressed 42% more actin per cell than the control cells (P<0.05, Fig. 2D). Fibroblast size increased after TGF-β1 and bFGF treatment by 20% and 14%, respectively, relative to controls (P<0.05, Fig. 2E). Finally, F-actin expression per unit area was 67% and 55% greater in cells treated with TGF-β1 than in control cells and those treated with bFGF, respectively (P<0.05; Fig. 2F).

Effect of TGF-β1 treatment on α-SMA

All cells expressed detectable levels of α-SMA. Epifluorescence of α-SMA at low magnification (100× to 400×) was minimal (10 s exposure time) and difficult to quantify. However, water immersion at 600× magnification permitted visualization of structural α-SMA. Control cells exhibited a very diffuse α-SMA signal, and there was some evidence of structural α-SMA (Fig. 3A), but not to the same extent as cells treated with TGF-β1. bFGF-treated cells appeared to have high levels of α-SMA, but it was a highly diffuse signal and much of the fluorescence was likely the result of the aggregation of large numbers of fibroblasts in that treatment group (Fig. 3B). Fibroblasts treated with TGF-β1 expressed large amounts of structural α-SMA (Fig. 3C).

Vinculin and collagen

TGF-β1 treatment caused vinculin protein to increase 2.9-fold relative to control cells and 3-fold relative to cells incubated in bFGF (P<0.05; Fig. 4A). There was no effect of bFGF treatment on vinculin production in cardiac fibroblasts, compared with the control (P>0.05). There was no effect of either TGF-β1 or bFGF treatment on the level of collagen type I when compared with the control group (P>0.05, Fig. 4B).

MMP activity

In cells that had undergone apparent differentiation with the addition of TGF-β1, there was a 5.3-fold increase in gelatinase activity at the cleaved MMP site (~60 kDa) (P<0.05, Fig. 5B).

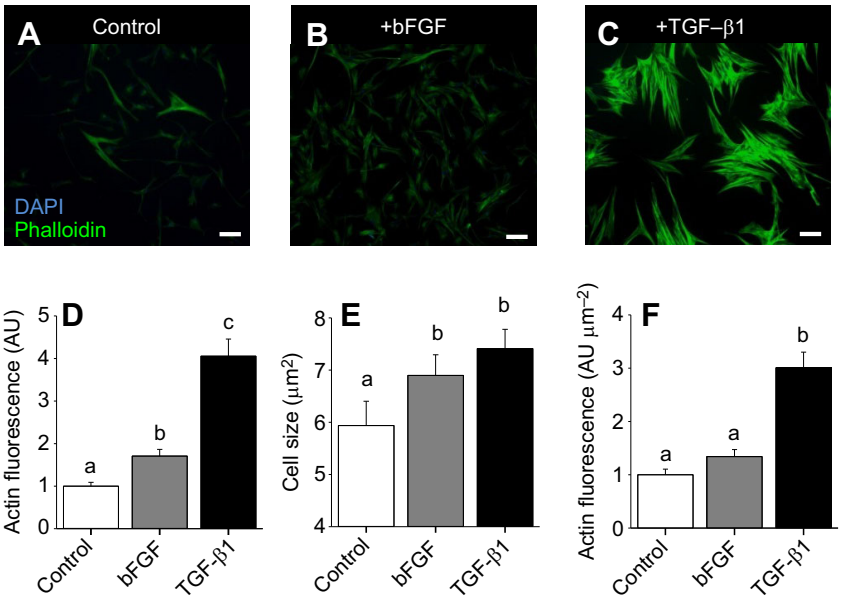

Fig. 2. Morphological changes in trout cardiac fibroblasts treated with bFGF or TGF-β1. (A–C) Representative micrographs showing fibroblasts at 100× magnification, stained for total filamentous actin after incubation for 7 days in control medium, or medium containing bFGF or TGF-β1. Cells were stained with Alexa 488-conjugated phalloidin for 30 min and counterstained with DAPI. Scale bars: 50 μm. (D–F) Cell area, total F-actin fluorescence and F-actin fluorescence per μm^2 of cell area were quantified using densitometry. (D) Mean F-actin signal per fibroblast. (E) Mean area of fibroblasts. (F) Mean F-actin per unit area. Letters denote significance at α=0.05. *n*=80–100 individual cells from three cell lines generated from three different fish.

Journal of Experimental Biology (2018) 221, jeb189167. doi:10.1242/jeb.189167

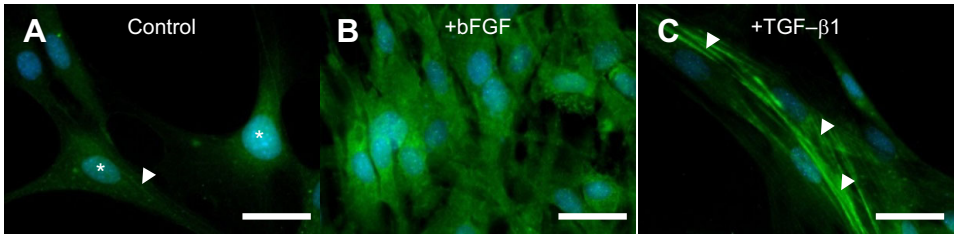

Fig. 3. Effect of bFGF and TGF-β1 treatment of trout cardiac fibroblasts on α-smooth muscle actin. (A–C) Micrographs of cardiac fibroblasts treated with bFGF and TGF-β1, and stained for alpha-smooth muscle actin protein (α-SMA) specifically. α-SMA signal was weak at 100× to 400× magnification (barely detectable under exposure settings >10 s) and could not be quantified as F-actin was. However, α-SMA could be visualized under 600× water immersion. (A) Fibroblasts maintained in control medium demonstrated slight α-SMA organization (white arrowheads) coupled with diffuse signal. (B) bFGF-treated fibroblasts did not possess any structural α-SMA, but aggregated in high numbers with diffuse actin signal. (C) Fibroblasts treated with TGF-β1 demonstrated multiple highly organized α-SMA filaments spanning the cells (white arrowheads). *n*=3, with each *n* being a protein sample extracted from cultured cells derived from a different trout ventricle. Scale bars: 20 μm.

bFGF did not affect gelatinase activity. Gelatinase activity in the medium from treated and control cells was not affected by treatment (P>0.05, Fig. 5C). It is not known if the gelatinase activity is from MMP-2, MMP-9 or a combination of the two, as these two proteins only differ by ∼2 kDa in molecular mass. This difference was not distinguishable on the gels.

Expression of key collagen remodelling genes

The transcript abundance of *mmp-2* decreased by 43.7% in bFGF-treated cells (P<0.05, Fig. 6) but did not change with TGF-β1 treatment. bFGF and TGF-β1 treatment upregulated *mmp-9* expression 4.2- and 3.1-fold, respectively. These increases in transcript abundance were significantly greater than control cells (P<0.05), but the difference in *mmp-9* expression was not different between bFGF- and TGF-β1-treated cells (P>0.05). Expression of *timp-2* was increased 2.3-fold with bFGF treatment and 2.5-fold with TGF-β1 treatment (P<0.05). The transcript abundance of *col1a1* was increased 1.4-fold with TGF-β1 treatment, but was not affected by bFGF treatment (P<0.05).

DISCUSSION

This is the first study demonstrating that TGF-β1 treatment can cause cardiac fibroblasts from a fish species, to transform into apparent myofibroblasts. The results of this study also suggest that myofibroblasts, derived from fibroblasts, in response to TGF-β1, could be integral to the remodelling of the fish heart. The phosphorylation of Smad2 and subsequent increase in vinculin, gelatinase activity and structural α-SMA, as well as total filamentous actin, demonstrate that the response of fish fibroblasts to TGF-β1 could be similar to that characterized in fibroblasts from mammalian species. In addition, given what is known about the role of myofibroblasts during remodelling in mammalian hearts, the results of this study indicate that quantifying the presence and activity of myofibroblasts in the trout heart during thermal acclimation is a

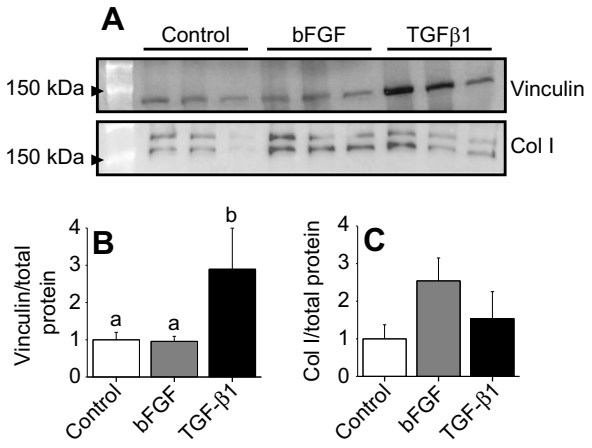

Fig. 4. Effect of TGF-β1 and bFGF treatment of trout cardiac fibroblasts on vinculin and collagen protein expression. The fibroblast cultures were treated with medium alone or medium containing 15 ng ml^{-1} bFGF or 15 ng ml^{-1} TGF-β1 daily for 7 days and vinculin and collagen were quantified by western blot and densitometry. (A) Western blot images of vinculin and collagen proteins from three cell lines from the ventricles of three different fish, treated with either bFGF or TGF-β1 and detected with mouse anti-vinculin or rabbit anti-salmon collagen type I antibodies. Blots are from membranes acquired from two different gels that separated the same samples. Mean (B) vinculin and (C) collagen levels measured by densitometry and standardized to total protein in the same sample. Differences were detected using a one-way ANOVA with *post hoc* Bonferroni correction. Bars labelled with different letters are significantly different at α=0.05.

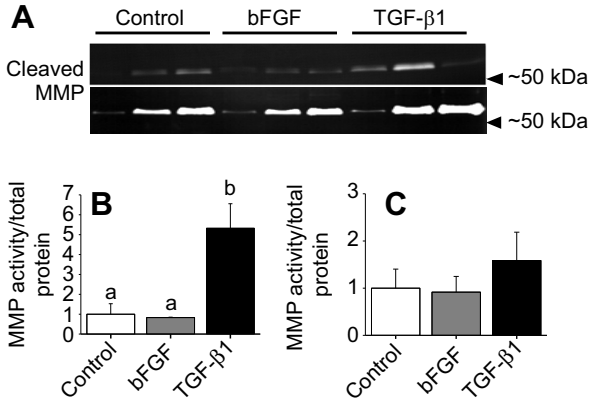

Fig. 5. Gelatin zymograms showing the influence of bFGF and TGF-β1 treatment on the presence and activity of gelatinases in trout cardiac fibroblast cultures. Spent, undiluted medium and protein extracted from pelleted cells treated on alternating days with bFGF and TGF-β1 for 7 days were resolved on a 9% polyacrylamide gel with 0.2% w/v gelatin under non-heated, non-reducing conditions. Enzymes were renatured in 2.5% Triton X-100 and allowed to digest gelatin in the gel for 36 h at 38°C in incubation buffer containing zinc. (A) Resulting gels stained with Coomassie Blue, where bands are sites of cleaved gelatinase digestion and relative activity was quantified using densitometry analysis. The top panel shows MMP activity from cell pellets, while the bottom panel is from medium samples. (B,C) Quantification of gelatinase activity relative to total protein in the same lane in (B) cell pellets and (C) whole medium. Letters denote a significant effect (P<0.05) of treatment on gelatinase activity. *n*=3, with each *n* being a different population of cells, thawed from a different cryovial on a different day.

Journal of Experimental Biology (2018) 221, jeb189167. doi:10.1242/jeb.189167

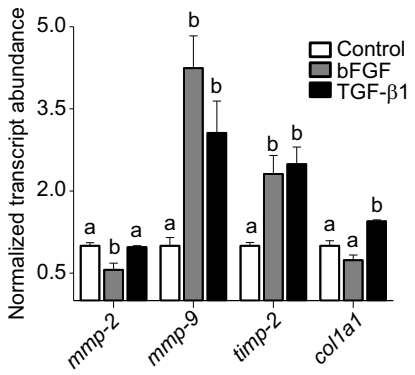

Fig. 6. Effect of bFGF and TGF-β1 treatment of trout cardiac fibroblasts on the expression of genes involved in ECM regulation. Transcript abundance for control, and bFGF- and TGF-β1-treated cells after 7 days of treatment. The amount of transcript (*mmp-2*, *mmp-9*, *timp-2*, *col1a1*) in bFGF and TGF-β1 groups are relative to the control group, which is set to 1 for each gene. mRNA level for each gene was normalized to the transcript abundance of *β-actin*. Letters denote a significant effect ($P<0.05$) of treatment on transcript abundance, relative to control. $n=3$, with each n being a different population of cells, thawed from a different cryovial on a different day.

viable new endpoint to characterize the cardiac remodelling response. This study also establishes the use of pSmad2 and vinculin as markers for the activation of the TGF-β1 pathway, which has not yet been examined *in vivo* in the rainbow trout heart. Finally, the use of fish cell lines in this research has provided novel insight into the role of TGF-β1 in regulating the activity and fate of cardiac fibroblasts in the fish heart, and also demonstrates the usefulness of cell culture studies in characterizing critical cellular pathways.

Smad2 activation

Smad2 is directly linked to the TGF-β1 receptor as it becomes phosphorylated in response to TGF-β1 binding and translocates to the nucleus, leading to changes in gene expression (Nyati, 2012). The change in gene expression patterns observed in the current study are similar to that previously reported (Johnston and Gillis, 2017), in that there was an increase in expression of *mmp-9*, *timp-2* and *col1a1* transcripts in response to TGF-β1. However, we have previously demonstrated that TGF-β1 treatment of trout cardiac fibroblasts caused a decrease in *mmp-2* (Johnston and Gillis, 2017), whereas in the current study there was no change in *mmp-2* expression. Furthermore, in our previous study, we found an increase in collagen type I protein (Johnston and Gillis, 2017) in TGF-β1-treated trout cardiac fibroblasts, but no change in cell morphology, while in the current study there was no increase in collagen but we noted a change in cell morphology. One explanation for the different results between these two studies is that there is a dose-dependent response of the fibroblasts to TGF-β1, with a single dose promoting collagen synthesis, and repetitive doses triggering differentiation. This may have to do with the level of Smad2 phosphorylation, which was not previously examined, but would be an important next step for future studies examining where the threshold between collagen synthesis and degradation occurs in response to TGF-β1. In the mammalian heart, an increase in Smad2 phosphorylation can occur during pressure-induced cardiac remodelling in response to hypertension and/or myocardial infarction (Bjørnstad et al., 2012; Euler-Taimor and Heger, 2006; Xia et al., 2009). It has been suggested that the workload on the trout heart increases during cold acclimation as a result of an increase in vascular resistance caused by an increase in blood viscosity (Farrell, 1984; Graham and Farrell, 1989; Graham and Fletcher, 1985). Such an increase in workload has the potential to increase the biomechanical forces on the myocardium, and as a result, trigger an increase in TGF-β1 production by the trout fibroblasts (Johnston and Gillis, 2017). In the current study, we demonstrate that TGF-β1 treatment causes an increase in Smad2 phosphorylation. Since TGF-β1 protein is difficult to quantify *in vivo* because of its transient nature, pSmad2 may be a suitable proxy in future studies that investigate whether TGF-β1 signalling increases in the trout myocardium during cold acclimation.

Effect of TGF-β1 and bFGF on cellular morphology and protein expression

Only cells treated with TGF-β1 contained multiple strands of highly organized, striated α-SMA in the cytoskeleton. This feature was the most obvious indication of myofibroblast differentiation. Other evidence of myofibroblast differentiation, caused by TGF-β1 treatment, was the increase in vinculin, a protein that anchors intracellular actin filaments to the extracellular domain, thus maintaining the integrity of the connections bridging intracellular components and the ECM. This response is likely linked to the increase in contractile α-SMA, where the presence of vinculin would be necessary for maintaining cellular adhesion in the face of increased mechanical force within an intact heart. Experiments with rats demonstrate that vinculin levels in the cardiac fibroblasts increase in response to mechanical overload of the heart (Sharp et al., 1997). If cold acclimation causes fibroblasts in the trout heart to be exposed to greater mechanical force, then an increase in vinculin protein would be indicative of the cellular response to this physiological stressor.

Both TGF-β1 and bFGF increased the total area occupied by individual cells; however, only TGF-β1 increased both cell size and the amount of F-actin in the cells. This suggests that treatment with TGF-β1 results in more actin per cell, which could contribute to elevated contractile function (Dominguez and Holmes, 2011). Furthermore, myofibroblasts are also larger *in vitro* as well as *in vivo*, and are present in the hypertrophied mammalian heart. It would therefore be of interest to determine whether they are present in the remodelled trout myocardium (Herum et al., 2017).

In the current study, the increase in the size of fibroblasts when treated with bFGF may be attributed to the increase in filopodia branching and length associated with bFGF treatment, as has been demonstrated in artery, neuron and airway development (Fernandez et al., 2000; Placzek and Skaer, 1999; Szebenyi et al., 2001). bFGF also plays an important role in wound healing and remodelling, where its signal stimulates angiogenesis and inhibits myofibroblast differentiation in the heart (Fedak et al., 2012; Shao et al., 2006; Wang et al., 2016). Since rainbow trout cardiac fibroblasts responded to bFGF in this study, it is possible that this signalling factor also plays a role in the trout heart during thermal acclimation.

MMP activity and gene expression

Our result demonstrating a lack of change in the level of collagen type I in cells treated with TGF-β1 is in conflict with previous studies demonstrating that mammalian myofibroblasts treated with TGF-β1 increase collagen protein expression (Baum and Duffy, 2011; Hinz, 2007). This finding prompted the measurement of MMP activity, because while collagen may have been produced in greater quantity in differentiated cells, it could also have been hydrolysed at the same rate. The 5.3-fold increase in ∼60 kDa gelatinase activity in TGF-β1-treated cells could be responsible, at

least in part, for the lack of change seen in collagen protein, despite an increase in *col1a1* expression. Enhanced MMP-2 activity in cardiac myofibroblasts has been demonstrated in the post-infarct mammalian heart (Riches et al., 2009; Turner and Porter, 2012). While gelatinases do not typically cleave the collagen triple helix directly, their activity is indicative of matrix degradation during the remodelling process (Riley et al., 2002). As MMP-2 and MMP-9 are of similar molecular mass in trout, it is not known which of these is responsible for the measured increase in gelatinase activity. bFGF treatment decreased *mmp*-2 expression, whereas TGF-β1 increased the transcript abundance of *mmp-2*. Furthermore, the treatment of cells with bFGF and TGF-β1 caused an increase in the expression of *timp-2*. In the cell, TIMP-2 complexes with inactive proMMP-2 to aid in forming the active cleaved MMP-2 enzyme (Wang et al., 2000). Thus, it is possible that the observed enzyme in our study was MMP-2 if TIMP-2 acted as an activator in the TGF-β1-treated cells. Furthermore, MMP-2 can sometimes degrade native collagen type I, which could also explain why there was a decrease in this protein in cells treated with TGF-β1 (Messaritou et al., 2009).

Significance and perspectives

The remodelling of organs and tissues *in vivo* is a highly complex and tightly regulated process (Li and Weisel, 2014; Lu et al., 2011). The increase in cardiac collagen that occurs in the trout heart with cold acclimation may not result from a simple increase in collagen synthesis, but could also require the breakdown of existing ECM via MMP activity to ensure that the resulting biomechanical properties of myocardium are functionally appropriate. Furthermore, it is not known if cold acclimation causes a change in the type of collagen (type I versus type III) expressed in the rainbow trout heart. We have recently demonstrated that cold acclimation of zebrafish causes a decrease in the amount of thick collagen (type I) fibres, resulting in a higher thin:thick fibre ratio as well as a decrease in total collagen (Johnson et al., 2014). This large-scale change would require the breakdown of pre-existing collagen, possibly as a result of MMP activity. The results of the current study suggest that myofibroblasts, derived from fibroblasts, in response to TGF-β1, could be integral to this transformative process. In addition, these studies help to establish the utility of using the trout heart, as well as fish heart cell lines, as models to study cardiac ECM remodelling in vertebrates to gain further insight into this complex phenotypic response to a change in physiological conditions. Finally, among vertebrates, several cell types, in addition to fibroblasts/myofibroblasts, participate in this process. One such cell type in the mammalian heart are endothelium cells, which produce endothelin, which in turn regulates cardiac fibrosis (Hocher et al., 1999). Recently, a heart endothelial cell line, ASHe, was established from the Atlantic salmon (Pham et al., 2017). A future study that integrates these cells with the fibroblasts used in the current study, would enable a more complex investigation of the cellular interactions that regulate cardiac remodelling of fish.

Acknowledgements

The authors would like to thank Dr N. Vo (Waterloo) and Dr L. Lee (University of the Fraser Valley) for technical advice on this project, as well as acknowledge the efforts of three anonymous reviewers.

Competing interests

The authors declare no competing or financial interests.

Author contributions

Conceptualization: E.F.J., T.E.G.; Methodology: E.F.J., T.E.G.; Investigation: E.F.J.; Writing - original draft: E.F.J., T.E.G.; Writing - review & editing: E.F.J., T.E.G.; Supervision: T.E.G.; Project administration: T.E.G.; Funding acquisition: T.E.G.

Funding

This work was supported by a Discovery Grant, and a Discovery Accelerator Supplement, from the Natural Sciences and Engineering Research Council of Canada to T.E.G.

Supplementary information

Supplementary information available online at
http://jeb.biologists.org/lookup/doi/10.1242/jeb.189167.supplemental

References

Baum, J. and Duffy, H. S. (2011). Fibroblasts and myofibroblasts: what are we talking about? *J. Cardiovasc. Pharmacol.* **57**, 376-379.
Bjørnstad, J. L., Skrbic, B., Marstein, H. S., Hasic, A., Sjaastad, I., Louch, W. E., Florholmen, G., Christensen, G. and Tønnessen, T. (2012). Inhibition of SMAD2 phosphorylation preserves cardiac function during pressure overload. *Cardiovasc. Res.* **93**, 100-110.
Chablais, F. and Jazwinska, A. (2012). The regenerative capacity of the zebrafish heart is dependent on TGFbeta signaling. *Development* **139**, 1921-1930.
Darby, I. A., Laverdet, B., Bonte, F. and Desmouliere, A. (2014). Fibroblasts and myofibroblasts in wound healing. *Clin. Cosmet. Investig. Dermatol.* **7**, 301-311.
Dominguez, R. and Holmes, K. C. (2011). Actin structure and function. *Annu. Rev. Biophys.* **40**, 169-186.
Eaton, S. L., Roche, S. L., Llavero Hurtado, M., Oldknow, K. J., Farquharson, C., Gillingwater, T. H. and Wishart, T. M. (2013). Total protein analysis as a reliable loading control for quantitative fluorescent Western blotting. *PLoS ONE* **8**, e72457.
Euler-Taimor, G. and Heger, J. (2006). The complex pattern of SMAD signaling in the cardiovascular system. *Cardiovasc. Res.* **69**, 15-25.
Farrell, A. P. (1984). A review of cardiac performance in the teleost heart: intrinsic and humoral regulation. *Can. J. Zool.* **62**, 523-536.
Fedak, P. W. M., Bai, L., Turnbull, J., Ngu, J., Narine, K. and Duff, H. J. (2012). Cell therapy limits myofibroblast differentiation and structural cardiac remodeling: basic fibroblast growth factor-mediated paracrine mechanism. *Circ. Heart Fail.* **5**, 349-356.
Fernandez, B., Buehler, A., Wolfram, S., Kostin, S., Espanion, G., Franz, W. M., Niemann, H., Doevendans, P. A., Schaper, W. and Zimmermann, R. (2000). Transgenic myocardial overexpression of fibroblast growth factor-1 increases coronary artery density and branching. *Circ. Res.* **87**, 207-213.
Gillis, T. E. and Johnston, E. F. (2017). Cardiac preconditioning, remodelling and regeneration. In *The Cardiovascular System: Design, Control and Function*. Fish Physiology Book Series, Vol. 36A (ed. A. K. Gamperl, T. E. Gillis, A. P. Farrell and C. J. Brauner), pp. 185-233. Elsevier.
Gonzalez-Rosa, J. M., Martin, V., Peralta, M., Torres, M. and Mercader, N. (2011). Extensive scar formation and regression during heart regeneration after cryoinjury in zebrafish. *Development* **138**, 1663-1674.
Graham, M. S. and Fletcher, G. L. (1985). On the low viscosity blood of 2 cold water, marine sculpins - a comparison with the winter flounder. *J. Comp. Physiol. B* **155**, 455-459.
Graham, M. S. and Farrell, A. P. (1989). The effect of temperature acclimation and adrenaline on the performance of a perfused trout heart. *Physiol. Zool.* **62**, 38-61.
Herum, K. M., Lunde, I. G., McCulloch, A. D. and Christensen, G. (2017). The soft- and hard-heartedness of cardiac fibroblasts: mechanotransduction signaling pathways in fibrosis of the heart. *J. Clin. Med.* **6**, 1-50.
Hinz, B. (2007). Formation and function of the myofibroblast during tissue repair. *J. Invest. Dermatol.* **127**, 526-537.
Hocher, B., George, I., Rebstock, J., Bauch, A., Schwarz, A., Neumayer, H.-H. and Bauer, C. (1999). Endothelin system-dependent cardiac remodeling in renovascular hypertension. *Hypertension* **33**, 816-822.
Jester, J. V., Barry-Lane, P. A., Cavanagh, H. D. and Petroll, W. M. (1996). Induction of alpha-smooth muscle actin expression and myofibroblast transformation in cultured corneal keratocytes. *Cornea* **15**, 505-516.
Johnson, A. C., Turko, A. J., Klaiman, J. M., Johnston, E. F. and Gillis, T. E. (2014). Cold acclimation alters the connective tissue content of the zebrafish (Danio rerio) heart. *J. Exp. Biol.* **217**, 1868-1875.
Johnston, E. F. and Gillis, T. E. (2017). Transforming growth factor beta-1 (TGF-beta1) stimulates collagen synthesis in cultured rainbow trout cardiac fibroblasts. *J. Exp. Biol.* **220**, 2645-2653.
Keen, A. N., Fenna, A. J., McConnell, J. C., Sherratt, M. J., Gardner, P. and Shiels, H. A. (2016). The dynamic nature of hypertrophic and fibrotic remodeling of the fish ventricle. *Front. Physiol.* **6**, 427.
Keen, A. N., Klaiman, J. M., Shiels, H. A. and Gillis, T. E. (2017). Temperature-induced cardiac remodelling in fish. *J. Exp. Biol.* **220**, 147-160.
Khouw, I. M. S. L., van Wachem, P. B., Plantinga, J. A., Vujaskovic, Z., Wissink, M. J. B., de Leij, L. F. M. H. and van Luyn, M. J. A. (1999). TGF-beta and bFGF affect the differentiation of proliferating porcine fibroblasts into myofibroblasts in vitro. *Biomaterials* **20**, 1815-1822.
Klaiman, J. M., Fenna, A. J., Shiels, H. A., Macri, J. and Gillis, T. E. (2011). Cardiac remodeling in fish: strategies to maintain heart function during temperature Change. *PLoS ONE* **6**, e24464.

Klingberg, F., Hinz, B. and White, E. S. (2013). The myofibroblast matrix: implications for tissue repair and fibrosis. *J. Pathol.* **229**, 298-309.
Lee, K.-S., Hong, S.-H. and Bae, S.-C. (2002). Both the Smad and p38 MAPK pathways play a crucial role in Runx2 expression following induction by transforming growth factor-beta and bone morphogenetic protein. *Oncogene* **21**, 7156-7163.
Li, R. K. and Weisel, R. D. (2014). *Cardiac Regeneration and Repair: Biomaterials and Tissue Engineering*. Elsevier Science.
Lighthouse, J. K. and Small, E. M. (2016). Transcriptional control of cardiac fibroblast plasticity. *J. Mol. Cell. Cardiol.* **91**, 52-60.
Lødemel, J. B. and Olsen, R. L. (2003). Gelatinolytic activities in muscle of Atlantic cod (Gadus morhua), spotted wolffish (Anarhichas minor) and Atlantic salmon (*Salmo salar*). *J. Sci. Food Agric.* **83**, 1031-1036.
Lu, P., Takai, K., Weaver, V. M. and Werb, Z. (2011). Extracellular matrix degradation and remodeling in development and disease. *Cold Spring Harb. Perspect. Biol.* **3**, a005058.
Ma, Y., de Castro Bras, L. E., Toba, H., Iyer, R. P., Hall, M. E., Winniford, M. D., Lange, R. A., Tyagi, S. C. and Lindsey, M. L. (2014). Myofibroblasts and the extracellular matrix network in post-myocardial infarction cardiac remodeling. *Pflugers Arch.* **466**, 1113-1127.
Marro, J., Pfefferli, C., de Preux Charles, A.-S., Bise, T. and Jaźwińska, A. (2016). Collagen XII contributes to epicardial and connective tissues in the zebrafish heart during ontogenesis and regeneration. *PLoS ONE* **11**, e0165497.
Masur, S. K., Dewal, H. S., Dinh, T. T., Erenburg, I. and Petridou, S. (1996). Myofibroblasts differentiate from fibroblasts when plated at low density. *Proc. Natl. Acad. Sci. USA* **93**, 4219-4223.
Mattey, D. L., Dawes, P. T., Nixon, N. B. and Slater, H. (1997). Transforming growth factor beta 1 and interleukin 4 induced alpha smooth muscle actin expression and myofibroblast-like differentiation in human synovial fibroblasts in vitro: modulation by basic fibroblast growth factor. *Ann. Rheum. Dis.* **56**, 426-431.
Messaritou, G., East, L., Roghi, C., Isacke, C. M. and Yarwood, H. (2009). Membrane type-1 matrix metalloproteinase activity is regulated by the endocytic collagen receptor Endo180. *J. Cell Sci.* **122**, 4042-4048.
Nakao, A., Imamura, T., Souchelnytskyi, S., Kawabata, M., Ishisaki, A., Oeda, E., Tamaki, K., Hanai, J., Heldin, C. H., Miyazono, K. et al. (1997). TGF-beta receptor-mediated signalling through Smad2, Smad3 and Smad4. *EMBO J.* **16**, 5353-5362.
Nyati, M. K. (2012). Molecular imaging of TGF beta-induced Smad2/3 phosphorylation reveals a role for receptor tyrosine kinases in modulating TGF beta signaling (vol 17, pg 7424, 2011). *Clin. Cancer Res.* **18**, 2115-2115.
Pham, P. H., Vo, N. T. K., Tan, E. J. H., Russell, S., Jones, G., Lumsden, J. S. Bols, N. C. (2017). Development of an Atlantic salmon heart endothelial cell line (ASHe) that responds to lysophosphatidic acid (LPA). *In Vitro Cell. Dev. Biol. Anim.* **53**, 20-32.
Placzek, M. and Skaer, H. (1999). Airway patterning: a paradigm for restricted signalling. *Curr. Biol.* **9**, R506-R510.
Riches, K., Morley, M. E., Turner, N. A., O'Regan, D. J., Ball, S. G., Peers, C. and Porter, K. E. (2009). Chronic hypoxia inhibits MMP-2 activation and cellular invasion in human cardiac myofibroblasts. *J. Mol. Cell. Cardiol.* **47**, 391-399.
Riley, G. P., Curry, V., DeGroot, J., van El, B., Verzijl, N., Hazleman, B. L. and Bank, R. A. (2002). Matrix metalloproteinase activities and their relationship with collagen remodelling in tendon pathology. *Matrix Biol.* **21**, 185-195.
Ronnov-Jessen, L. and Petersen, O. W. (1993). Induction of alpha-smooth muscle actin by transforming growth factor-beta 1 in quiescent human breast gland fibroblasts. Implications for myofibroblast generation in breast neoplasia. *Lab. Invest.* **68**, 696-707.
Shao, Z.-Q., Takaji, K., Katayama, Y., Kunitomo, R., Sakaguchi, H., Lai, Z.-F. and Kawasuji, M. (2006). Effects of intramyocardial administration of slow-release basic fibroblast growth factor on angiogenesis and ventricular remodeling in a rat infarct model. *Circ. J.* **70**, 471-477.
Sharp, W. W., Simpson, D. G., Borg, T. K., Samarel, A. M. and Terracio, L. (1997). Mechanical forces regulate focal adhesion and costamere assembly in cardiac myocytes. *Am. J. Physiol.* **273**, H546-H556.
Sun, Y. and Weber, K. T. (1996). Angiotensin-converting enzyme and wound healing in diverse tissues of the rat. *J. Lab. Clin. Med.* **127**, 94-101.
Szebenyi, G., Dent, E. W., Callaway, J. L., Seys, C., Lueth, H. and Kalil, K. (2001). Fibroblast growth factor-2 promotes axon branching of cortical neurons by influencing morphology and behavior of the primary growth cone. *J. Neurosci.* **21**, 3932-3941.
Tomasek, J. J., Gabbiani, G., Hinz, B., Chaponnier, C. and Brown, R. A. (2002). Myofibroblasts and mechano-regulation of connective tissue remodelling. *Nat. Rev. Mol. Cell Biol.* **3**, 349-363.
Turner, N. A. and Porter, K. E. (2012). Regulation of myocardial matrix metalloproteinase expression and activity by cardiac fibroblasts. *IUBMB Life* **64**, 143-150.
Vaughan, M. B., Howard, E. W. and Tomasek, J. J. (2000). Transforming growth factor-beta1 promotes the morphological and functional differentiation of the myofibroblast. *Exp. Cell Res.* **257**, 180-189.
Visse, R. and Nagase, H. (2003). Matrix metalloproteinases and tissue inhibitors of metalloproteinases: structure, function, and biochemistry. *Circ. Res.* **92**, 827-839.
Wang, Z., Juttermann, R. and Soloway, P. D. (2000). TIMP-2 is required for efficient activation of proMMP-2 in vivo. *J. Biol. Chem.* **275**, 26411-26415.
Wang, B., Ma, X., Zhao, L., Zhou, X., Ma, Y., Sun, H., Yang, Y. and Chen, B. (2016). Injection of basic fibroblast growth factor together with adipose-derived stem cell transplantation: improved cardiac remodeling and function in myocardial infarction. *Clin. Exp. Med.* **16**, 539-550.
Xia, Y., Lee, K., Li, N., Corbett, D., Mendoza, L. and Frangogiannis, N. G. (2009). Characterization of the inflammatory and fibrotic response in a mouse model of cardiac pressure overload. *Histochem. Cell Biol.* **131**, 471-481.